

Ballistic magnetotransport in graphene

Ke Wang^{1,*} and T. A. Sedrakyan^{1,†}

¹*Department of Physics, University of Massachusetts, Amherst, MA 01003, USA*

(Dated: October 11, 2021)

We report that a perpendicular magnetic field introduces an anomalous interaction correction, $\delta\sigma$, to the static conductivity of doped graphene in the ballistic regime. The correction implies that the magnetoresistance, $\delta\rho_{xx}$ scales inversely with temperature $\delta\rho_{xx}(T) \propto 1/T$ in a parametrically large interval. When the disorder is scalar-like, the $\propto 1/T$ behavior is the leading contribution in the crossover between diffusive regime exhibiting weak localization and quantum magnetooscillations. The behavior originates from the field-induced breaking of the chiral symmetry of Dirac electrons around a single valley. The result is specific for generic two-dimensional Dirac materials which deviate from the half-filling. We conclude by proposing magnetotransport experiments, which have the capacity to detect the nature of impurities and defects in high-mobility Dirac monolayers such as recently fabricated ballistic graphene samples.

Introduction. Two well-established regimes characterize low-temperature magnetoresistance in a two-dimensional metallic system: Weak localization^{1,2} (WL) and Shubnikov–de Haas (SdH) oscillations. WL dominates in the low field limit $\omega_0\tau < (k_F L)^{-1}$. Here ω_0 is the cyclotron-frequency, τ is the impurity scattering time, and $L = v_F\tau$ is the mean free path. This regime is reached when the magnetic flux threading the area $L^2/2$ is smaller than the flux quantum^{3,4}. In the high field limit $\omega_0\tau > 1$, the spectrum is fully quantized into the Landau levels, and SdH oscillations become the dominating effect. The crossover between two limits is $(k_F L)^{-1} < \omega_0\tau < 1$, where the magnetic field B is non-quantizing. In this regime, the electron-electron interaction (EEI) are believed to play a significant role⁵. Namely, the interaction correction to the conductivity induce the B -dependence in the resistivity via the relation,

$$\delta\rho_{int} \simeq \rho_0^2(\omega_0^2\tau^2 - 1)\delta\sigma_{int}. \quad (1)$$

Here ρ_0 is the Drude resistivity and $\delta\sigma_{int}$ is the interaction correction to the longitudinal conductivity.

At the non-quantizing regime, magnetoresistance in the doped graphene has been widely studied in experiments^{6–10} in the last decade while theoretical investigations are still absent. One may expect that the B -dependence in $\delta\rho_{int}$ is simply product of $\rho^2\omega_0^2\tau^2$ and zero field performance in $\delta\sigma_{int}$. However, it is not the complete story. We have shown that the non-quantizing field on Dirac electrons has non-trivial effects on FO¹¹ and many-body physics¹².

In this letter, we report that $\delta\sigma_{int}$ itself can carry field-dependent corrections and thus leads to non-trivial magnetoresistance in graphene. In the ballistic regime $T\tau > 1$ of the doped graphene^{10,13}, we find

$$\delta\sigma_{int} \simeq \lambda_0 \frac{e^2\tau}{\pi} \left(tT - p \frac{\omega_0^2}{48T} \right). \quad (2)$$

Here λ_0 is the dimensionless interaction parameter, and t, p are dimensionless parameters determined by the disorder potential. Information about t and p can be extracted

from the zero-bias anomaly^{12,14} of tunneling density of states. The correction is present in a wide parameter range, where $\max(\omega_0, \tau^{-1}) < T < E_F$. Here E_F is the Fermi energy. From Eq. 1, the field-dependent correction to the resistivity reads¹⁵,

$$\delta\rho_{int}(B) - \delta\rho_{int}(0) \simeq \lambda_0\omega_0^2 \frac{e^2\tau^2\rho_0^2}{\pi} \left(tT\tau + \frac{p}{48T\tau} \right). \quad (3)$$

Temperature dependence of magnetoresistance in Eq. 3 highly depends on the ratio, p/t , of two disorder parameters that will be defined below. Generally, the ratio p/t can be any real number larger than $-1/2$. One prominent case is the scalar-like disorder potential, for which p/t is $\rightarrow +\infty$. To ensure the second term is not always sub-leading, we will focus on $p/t > 1$, where the disorder can be regarded as a perturbation around a scalar-like potential. When $1 < T\tau < \sqrt{p/t}$, the temperature dependence in magnetoresistance becomes reciprocal instead of being linear. Therefore, the parabolic curve in magnetoresistance becomes more flattened when T increases. See Fig. 1. Below, we present a qualitative explanation of the observed effect.

Qualitative discussion. Coherent scatterings off Friedel oscillations of electron density at distances $r \gg k_F^{-1}$ from an impurity renormalize the transport relaxation time. The coherent scattering is illustrated in Fig. 2. This process, leads to non-trivial temperature dependence^{16,17} in $\delta\sigma_{int}$. In two-dimensional electron gas (2DEG), $\delta\sigma_{int}$ is $\sim T\tau$ in the ballistic limit $T\tau > 1$ and $\sim \ln(T\tau)$ in the diffusive limit $T\tau < 1$.

Dirac nature of electrons in graphene^{18–30} can enrich the process of coherent scatterings because of the Berry phase π and chiral symmetry of Dirac electrons. Note that backscatterings off a single impurity can be classified into two types of Feynman diagrams. The first one is a loop type, giving Friedel oscillations. See inset (a) in Fig. 2. Here, the Berry phase π of Dirac electron leads to a faster decaying FO³¹. The second one is a vertex type diagram, yielding the correction to the density matrix. See inset (b) of Fig. 2. Here, the matrix structure of Dirac electron induces sensitivity of the vertex correction to the

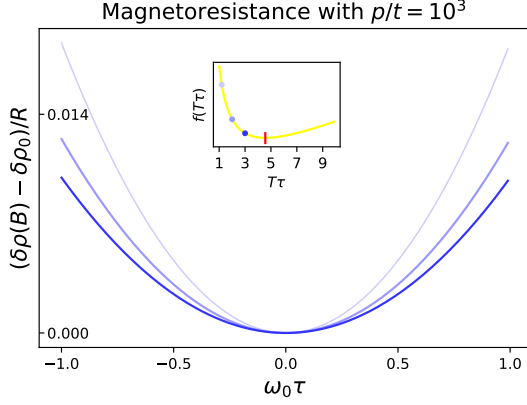


FIG. 1. Magnetoresistance, $[\delta\rho_{int}(B) - \delta\rho_{int}(0)]/R$, is plotted versus the dimensionless variable $\omega_0\tau$. The sign of $\omega_0\tau$ indicates the direction of the magnetic field and $R \equiv \lambda_0 e^2 \rho_0^2 / \pi$. Each curve correspond to the resistance plotted at a corresponding temperature shown by (blue) dots in the inset. From light to dark curves, the temperature is increasing while the curvature is decreasing. Values of temperature are pointed out in the inset. The inset depicts the function $f(T\tau) = tT\tau + p/48T\tau$ from Eq. 3. The (red) vertical bar locates the minimum of the function.

nature of disorder¹⁴. Two properties together lead to the well-known result that the temperature dependence in the conductivity in the ballistic limit is still $\sim T\tau$ but very sensitive to the disorder³¹. Importantly, if the disorder is scalar-like, the leading temperature behavior $\sim T\tau$ vanishes.

The presence of a weak magnetic field changes the scenario for both backscatterings in (a) and (b) from the inset of Fig. 2. The persistent FO emerges from loop correction¹¹,

$$\delta n(r) = \frac{gk_F}{2\pi^2 v_F r^2} \left[\frac{1}{k_F r} \cos\left(2k_F r - \frac{r^3}{12k_F l^4}\right) + 2\varphi^2(r) \sin\left(2k_F r - \frac{r^3}{12k_F l^4}\right) \right]. \quad (4)$$

Here the parameter g is defined in terms of the impurity potential, \hat{V}_r , as $g = \text{tr} \int d^2 r \hat{V}_r / 4$, $\varphi(r) = \omega_0 r / 2v_F$ and l is the magnetic length. The $\varphi(r)$ is the half of the angle of the arc, corresponding to the Dirac electron traveling from $\mathbf{0}$ to \mathbf{r} in a weak magnetic field. See Fig. 2. The value $\varphi(r)$ reflects the strength of chiral symmetry breaking semi-classically^{11,32}. A similar correction also emerges for the vertex correction¹².

As the next step, we will consider the transport relaxation time and see that the incorporation of $\varphi^2(r)$ into the estimate of the relaxation time can generate the correction in Eq. 2. It will help us to qualitatively extract the temperature behavior of magnetoconductivity from its relation to the transport time³³.

At first, let us estimate the relaxation time at zero-

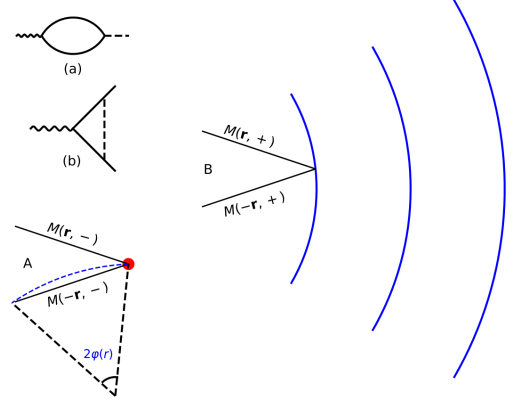


FIG. 2. Coherent scatterings between A and B paths: A is the path of backscattering off an impurity while B is the path when electrons hit the Friedel oscillations (or modulation of density matrix introduced by impurities), presented by blue curves. In the presence of a magnetic field, the path is curved, shown by the dashed arc. The angle of the arc is $2\varphi(r) = \omega_0 r / v_F$. Due to the Dirac nature of electrons, each propagator carries a matrix M . The inset plots two types of backscatterings off an impurity : (a) the loop type that creates Friedel oscillations. (b) the vertex type that creates correction to the density matrix.

field, where a linear temperature dependence emerges:

$$\frac{1}{\tau} = \int \frac{d\theta}{2\pi} (1 - \cos\theta) |f_0 + f_1(\theta)|^2. \quad (5)$$

Here f_0 and f_1 are respectively the scattering amplitudes off impurities and impurity-induced potentials. In the absence of the magnetic field, according to Refs. 17 and 34, the function f_1 can be cast as an integral $f_1(\theta) = \int dr F(r)$ and

$$F(r) = -\lambda_0 g \int_0^{+\infty} dr \frac{r_T}{\sinh r/r_T} \sin(2k_F r) J_0(qr). \quad (6)$$

Here $r_T = v_F / (2\pi T)$ is the thermal length, $|q| = 2k_F \sin\theta/2$ and J_0 is the zero Bessel function. The coefficient λ_0 is the dimensionless interaction parameter and the main contribution to Eq. 5 comes from the region $\theta \sim \pi$. One can expand $\theta = \pi + \delta\theta$ and $q \simeq 2k_F - k_F \delta\theta^2$. The condition $k_F \delta\theta^2 r_T \sim 1$ translates into $\delta\theta \sim (k_F r_T)^{-1/2}$. With the asymptotic expression of Bessel function, the power counting in the integral becomes $r^{-3/2}$ when $r < r_T$. When $\delta\theta < (k_F r_T)^{-1/2}$, the integral in Eq. 6, gives $\sim (k_F r_T)^{-1/2}$. Thus the integral in Eq. 5 is estimated by $(k_F r_T)^{-1}$. This indicates that the interaction correction to τ is proportional to T and the corresponding correction to $\delta\sigma_{int}$ is also linear in T .

In the presence of a magnetic field, the trajectories of electrons are curved, and the chiral symmetry of Dirac electrons is broken. Thus the suppressed backscattering is enhanced by the magnetic field. The incorporation of the symmetry-breaking effect leads to field-dependent correction to the scattering amplitude. Namely, $f_1 \rightarrow$

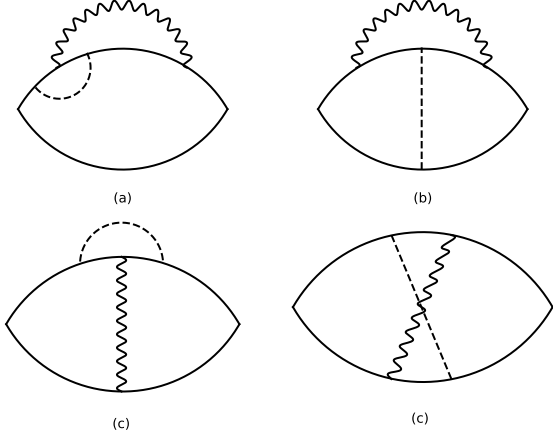


FIG. 3. Feynman diagrams giving leading field-dependent corrections to the longitudinal static conductivity. Solid lines represent the Feynman propagators. Dashed lines are the static impurities, while the wavy lines represent the electron-electron interactions.

$f_1 + \delta f_1$ and δf_1 is given by $\int dr F(r) \varphi^2(r)$. Here $\varphi^2(r)$ changes power counting to $r^{1/2}$ and the integral gives $\sim \omega_0^2 (k_F r_T)^{3/2}$. The θ -integral remains the same. Thus the field-dependent corrections to τ and $\delta\sigma_{int}$ are proportional to $\omega_0^2 T^{-1}$.

Below, we rigorously trace the current-current correlation function to derive the temperature-dependence in $\delta\sigma_{int}$.

Magnetoconductivity from Kubo formula. The static conductivity can be evaluated from the current-current correlation function³³. Namely, $\sigma_{\alpha,\beta} = \lim_{\omega \rightarrow 0} \frac{i}{\omega} \Pi_{\alpha,\beta}(\omega)$. Here the $\Pi_{\alpha,\beta}(\omega)$ is obtained by taking analytic continuation of current-current correlation function $\Pi_{\alpha,\beta}(i\Omega_n)$ via $i\Omega_n \rightarrow \omega$, $\Pi_{\alpha,\beta}(i\Omega_n) = \int_0^{1/T} d\tau \langle T_\tau \hat{j}_\alpha(\tau) \hat{j}_\beta(0) \rangle e^{i\Omega_n \tau}$. Here $\hat{j}_\alpha(\tau)$, $\alpha = 1, 2$, is the current operator at imaginary time τ , $\omega_n = 2\pi T n$ is the bosonic Matsubara frequency and $i\Omega_n \rightarrow \omega$ represents the analytic continuation.

At finite doping, one can treat impurity and interaction potential as the perturbation to \hat{H}_0 . Here H_0 is the Dirac Hamiltonian coupled to $U(1)$ gauge field,

$$\hat{H}_0 = v_F \int d^2 \mathbf{r} \hat{\Psi}^\dagger(\mathbf{r}) [\hat{\Sigma}_\alpha (-i\partial^\alpha + eA^\alpha)] \hat{\Psi}(\mathbf{r}). \quad (7)$$

Here α is summed in x and y , v_F is the Fermi velocity, $\hat{\Psi} = (\hat{\psi}_{AK}, \hat{\psi}_{BK}, \hat{\psi}_{BK'}, \hat{\psi}_{AK'})$ is the 4-component fermion operator and $\hat{\Sigma}_{x,y} = \hat{\tau}_z \otimes \hat{\sigma}_{x,y}$, where $\hat{\tau}_z$ is the third Pauli matrix acting in K, K' space and $\hat{\sigma}_{x,y}$ are Pauli matrices acting in the space of A, B sublattices. The gauge field is adopted by $\mathbf{A} = (-eBy, 0)$.

Now, we consider the Gaussian-correlated potential. Meanwhile, the symmetry-allowed disorder potential is described by five parameters^{35–37}, namely,

$$\langle \hat{V}_{\mathbf{r}} \otimes \hat{V}_{\mathbf{r}'} \rangle = \delta_{\mathbf{r},\mathbf{r}'} \left[\gamma_0 \hat{I} \otimes \hat{I} + g_i^m \hat{Q}_m^i \otimes \hat{Q}_m^i \right] \quad (8)$$

Here $\hat{V}_{\mathbf{r}}$ is the impurity potential and the bracket $\langle \dots \rangle$ is the average over impurity distributions. \hat{I} is the identity matrix. Here $\hat{Q}_m^i = \hat{\Sigma}_m \hat{\Lambda}_i$ and $\hat{\Sigma}_z = \hat{\tau}_0 \otimes \hat{\sigma}_z$, $\hat{\Lambda}_x = \hat{\tau}_x \otimes \hat{\sigma}_z$, $\hat{\Lambda}_y = \hat{\tau}_y \otimes \hat{\sigma}_z$, $\hat{\Lambda}_z = \hat{\tau}_z \otimes \hat{\sigma}_0$. We adopt the notation from Ref. 35, $g_z^z = \gamma_z$, $g_z^{x,y} = \gamma_\perp$, $g_{x,y}^z = \beta_z$ and $g_{x,y}^{x,y} = \beta_\perp$.

To illustrate coherent scattering quantitatively, we use the semiclassical expression of Dirac propagators in the real space¹², $\langle G(\mathbf{r}, \omega) \rangle \sim e^{i \text{sgn}(\omega) \Phi_0(r) - r/(2\tau v_F)} M(r, \text{sgn}(\omega)) / k_F r$. Here $\Phi_0(r)$ is the phase including both $k_F r$ and the magnetic phase³⁸. The form of matrix M shows that chiral-symmetry is broken in each valley but it is preserved in the Brillouin zone¹². The field-dependent part in M reads, $M - M_0 \simeq -\varphi^2(r) \hat{I} / 2 - i \text{sgn}(\omega) \varphi(r) \hat{\Sigma}_z$. Here M_0 is the value of matrix M in the absence of field and \hat{I} is the identity matrix.

Applying perturbations, one finds that series of Feynman diagrams led to dominant contributions to the conductivity. Up to the lowest orders of the impurity potential and interactions, we find that the diagrams in Fig. 3 give the leading field-dependent corrections to the longitudinal and static conductivity, $\delta\sigma_{xx}$. Namely, these are diagrams that contain vertex corrections¹², while others in the same order of perturbation theory are subleading.

The exact expression corresponding diagrams in Fig. 3 can be simplified. In the leading in $(T\tau)^{-1}$ order, and upon neglecting highly-oscillatory $\sim \exp i2k_F r$ terms, one arrives at a short expression for the conductivity correction³⁹,

$$\delta\sigma_{xx} \simeq -\lambda_0 \frac{e^2 \tau}{\pi^2 \alpha_{\text{tr}}} \int_0^{E_F} d\Omega \frac{d}{d\Omega} \left(\Omega \coth \frac{\Omega}{2T} \right) \text{Im} I(\Omega). \quad (9)$$

Here the function $I(\Omega)$ is expressed by the integral, $I(\Omega) = \int y^{-1} dy (2p' \varphi^2(y) + t') e^{2i(\Omega + i\tau)y/v_F}$, $\lambda_0 = k_F U_0 / 2\pi v_F$ is the dimensionless interaction constant at zero momentum. Parameters p' and t' are defined by $p' = \gamma_0 - \beta_z - \gamma_z$ and $t' = 2\gamma_z + 2\beta_z + \beta_\perp + \gamma_\perp$. The expression of $I(\Omega)$ originates from the coherent scatterings in Fig. 2. Notice the constant t' does not contain γ_0 , while p' , representing the enhancement of backscattering, depends on γ_0 . For short-ranged and weak scatterers, the parameter α_{tr} is found to be $\alpha_{\text{tr}} = \gamma_0 + 4\beta_\perp + 2\gamma_\perp + 2\beta_z + \gamma_z$, determining the Drude conductivity in graphene³⁷.

The integration in the expression of $\text{Im} I(\Omega)$ can be analytically performed, giving

$$\text{Im} I(\Omega) = \frac{\pi t}{2} + p \frac{(\omega_0 \tau)^2}{4} \frac{\Omega \tau}{(1 + \Omega^2 \tau^2)^2}. \quad (10)$$

The zero-field part shares the same integration as in Ref. 17. The linear T -dependence in $\delta\sigma_{xx}$ at the zero field is obtained from the property, $\lim_{\Omega \rightarrow 0} \Omega \coth \Omega / 2T \simeq 2T$. The sensitivity to the disorder potential in the zero-field limit, namely the sensitivity to parameter t , agrees well with the result in Ref. 31.

The field-dependent correction in Eq. 9 mainly originates from the region $0 < \Omega < 2T$. In this region,

one can linearize $\frac{d}{d\Omega} \left(\Omega \coth \frac{\Omega}{2T} \right) \simeq \Omega/3T$. Notice that the characteristic scale for Ω in Eq. 10 is $\sim \tau^{-1}$. The integral over Ω does not introduce extra temperature dependence. Thus the field-dependent correction $\delta\sigma_{xx}$ is $\sim \omega_0^2 T^{-1}$. Tracing the integral rigorously, one can obtain Eq. 2, where we define $t = t'/\alpha_{\text{tr}}$ and $p = p'/\alpha_{\text{tr}}$. Inverting the magnetoconductivity tensor gives us Eq. 3, which is the main result of the present work. The result is specific for Dirac electron and valid in a large parameter space when $\omega_0 < T < E_F$.

The present technological capabilities do not allow one to engineer the graphene samples with a given impurity type to the best of our knowledge. Therefore, the present theory allows extracting the information about the impurity in the sample from the magnetotransport measurement. Namely, upon fitting the temperature dependence of observed magnetoresistance with Eq. 3, one can extract the ratio of p/t . This helps to understand if the impurity in the given sample is mostly scalar type ($p/t \gg 1$) or mostly non-diagonal ($p/t \lesssim 1$).

Implications for the experiments. The new magnetoresistance behavior can be observed in experiments, provided with two conditions on disorders: (1). the disorder in the sample should ensure the inequality, $p/t \gg 1$. (2). Sample should be clean enough so that the ballistic transport can be observed.

To ensure $p/t \gg 1$, the type of disorders in a sample needs to be primarily scalar-like. Namely, only a small portion of disorder potentials create intra-valley scatter-

ings $A \leftrightarrow B$, intervalley scatterings $K \leftrightarrow K'$, and different on-site chemical potentials on sub-lattices.

The ballistic transport sets a lower bound for temperature (from now on we restore k_B/\hbar prefactor in the expression for T), $T > T_0 = k_B/\hbar\tau$. Meanwhile, the temperature should be low enough so that the thermal effects and phonon effects do not defeat the quantum effects of electrons. Thus sample should be clean enough for T_0 to represent a low temperature. In the previous magnetotransport experiments for, samples under consideration were not clean enough for the ballistic transport to be observed. For example, in Refs. 7 and 8, the mobility of sample is $\mu \sim 2 \times 10^3$ cm/Vs and the transport time is $\tau \sim 100$ fs. The temperature T_0 is $T_0 \sim 500K$. This is a high temperature where thermal, and phonon effects^{40–43} are strong and dominating. Nowadays, a clean sample with highly mobile electrons can be fabricated. According to Ref. 44, the method of chemical vapor deposition on reusable copper can be used to fabricate the graphene device with a high mobility, $\mu \sim 3.5 \times 10^5$ cm/Vs. The subsequent work¹³ shows that the electron mobility can be enhanced to be $\mu \sim 3 \times 10^6$ cm/Vs together with the observation of ballistic transport at 1.7K. These recent techniques may allow one to study the magnetoresistance of the doped graphene in the ballistic regime. In this regard, the predicted phenomenon in this letter can be observed.

Acknowledgments. We are grateful to M. E. Raikh for valuable discussions. The research was supported by startup funds from the University of Massachusetts, Amherst.

* kewang@umass.edu

† tsedrakyan@umass.edu

¹ Shinobu Hikami, Anatoly I. Larkin, and Yosuke Nagaoka, “Spin-Orbit Interaction and Magnetoresistance in the Two Dimensional Random System,” *Progress of Theoretical Physics* **63**, 707 (1980).

² B. L. Altshuler, D. Khmel'nitzkii, A. I. Larkin, and P. A. Lee, “Magnetoresistance and hall effect in a disordered two-dimensional electron gas,” *Phys. Rev. B* **22**, 5142 (1980).

³ M.I. Dyakonov, “Magnetoconductance due to weak localization beyond the diffusion approximation: The high-field limit,” *Solid State Communications* **92**, 711 (1994).

⁴ A. Cassam-Chenai and B. Shapiro, “Two dimensional weak localization beyond the diffusion approximation,” *J. Phys. I France* **4**, 1527 (1994).

⁵ T. A. Sedrakyan and M. E. Raikh, “Crossover from weak localization to shubnikov–de haas oscillations in a high-mobility 2d electron gas,” *Phys. Rev. Lett.* **100**, 106806 (2008).

⁶ A. A. Kozikov, A. K. Savchenko, B. N. Narozhny, and A. V. Shytov, “Electron-electron interactions in the conductivity of graphene,” *Phys. Rev. B* **82**, 075424 (2010).

⁷ B. Jouault, B. Jabakhanji, N. Camara, W. Desrat, C. Consejo, and J. Camassel, “Interplay between interferences

and electron-electron interactions in epitaxial graphene,” *Phys. Rev. B* **83**, 195417 (2011).

⁸ Johannes Jobst, Daniel Waldmann, Igor V. Gornyi, Alexander D. Mirlin, and Heiko B. Weber, “Electron-electron interaction in the magnetoresistance of graphene,” *Phys. Rev. Lett.* **108**, 106601 (2012).

⁹ B. Jabakhanji, D. Kazazis, W. Desrat, A. Michon, M. Portail, and B. Jouault, “Magnetoresistance of disordered graphene: From low to high temperatures,” *Phys. Rev. B* **90**, 035423 (2014).

¹⁰ K. Gopinadhan, Y. J. Shin, R. Jalil, T. Venkatesan, A. K. Geim, A. H. C. Neto, and H. Yang, “Extremely large magnetoresistance in few-layer graphene/boron–nitride heterostructures,” *Nature Communications* **6**, 8337 (2015).

¹¹ K. Wang, M. E. Raikh, and T. A. Sedrakyan, “Persistent friedel oscillations in graphene due to a weak magnetic field,” *Phys. Rev. B* **103**, 085418 (2021).

¹² K. Wang, M. E. Raikh, and T. A. Sedrakyan, “Interaction effects in graphene in a weak magnetic field,” *Phys. Rev. B* **104**, L161102 (2021).

¹³ L. Banszerus, M. Schmitz, S. Engels, M. Goldsche, K. Watanabe, T. Taniguchi, B. Beschoten, and C. Stampfer, “Ballistic transport exceeding 28 μm in cvd grown graphene,” *Nano Letters* **16**, 1387–1391 (2016).

¹⁴ E. Mariani, L. I. Glazman, A. Kamenev, and F. von Op-

- pen, “Zero-bias anomaly in the tunneling density of states of graphene,” *Phys. Rev. B* **76**, 165402 (2007).
- 15 One may notice that $\omega_0^2(T\tau)^{-1}$ dependence can also originate from the interaction correction to Hall coefficient. See PhysRevB.64.201201. Note that the disorder parameter before this correction is t and thus the correction is always sub-leading to $\omega_0^2(T\tau)$.
 - 16 A. Gold and V. T. Dolgoplov, “Temperature dependence of the conductivity for the two-dimensional electron gas: Analytical results for low temperatures,” *Phys. Rev. B* **33**, 1076 (1986).
 - 17 G. Zala, B. N. Narozhny, and I. L. Aleiner, “Interaction corrections at intermediate temperatures: Longitudinal conductivity and kinetic equation,” *Phys. Rev. B* **64**, 214204 (2001).
 - 18 A. H. Castro Neto, F. Guinea, N. M. R. Peres, K. S. Novoselov, and A. K. Geim, “The electronic properties of graphene,” *Rev. Mod. Phys.* **81**, 109 (2009).
 - 19 S. Das Sarma, S. Adam, E. H. Hwang, and E. Rossi, “Electronic transport in two-dimensional graphene,” *Rev. Mod. Phys.* **83**, 407 (2011).
 - 20 M. O. Goerbig, “Electronic properties of graphene in a strong magnetic field,” *Rev. Mod. Phys.* **83**, 1193 (2011).
 - 21 V. N. Kotov, B. Uchoa, V. M. Pereira, F. Guinea, and A. H. Castro Neto, “Electron-electron interactions in graphene: Current status and perspectives,” *Rev. Mod. Phys.* **84**, 1067 (2012).
 - 22 S. Maiti and T. A. Sedrakyan, “Composite fermion state of graphene as a haldane-chen insulator,” *Phys. Rev. B* **100**, 125428 (2019).
 - 23 D. Pan, H. Xu, and F. J. García de Abajo, “Anomalous thermodiffusion of electrons in graphene,” *Phys. Rev. Lett.* **125**, 176802 (2020).
 - 24 B. N. Narozhny, I. V. Gornyi, and M. Titov, “Hydrodynamic collective modes in graphene,” *Phys. Rev. B* **103**, 115402 (2021).
 - 25 G. Wagner, D. X. Nguyen, and S. H. Simon, “Transport properties of multilayer graphene,” *Phys. Rev. B* **101**, 245438 (2020).
 - 26 S. A. Mikhailov, “Nonperturbative quasiclassical theory of graphene photoconductivity,” *Phys. Rev. B* **103**, 245406 (2021).
 - 27 T. Zhu, M. Antezza, and J. S. Wang, “Dynamical polarizability of graphene with spatial dispersion,” *Phys. Rev. B* **103**, 125421 (2021).
 - 28 M. Kamada, V. Gall, J. Sarkar, M. Kumar, A. Laitinen, I. Gornyi, and P. Hakonen, “Strong magnetoresistance in a graphene corbino disk at low magnetic fields,” *Phys. Rev. B* **104**, 115432 (2021).
 - 29 B. Real, O. Jamadi, M. Milićević, N. Pernet, P. St-Jean, T. Ozawa, G. Montambaux, I. Sagnes, A. Lemaître, L. Le Gratiet, A. Harouri, S. Ravets, J. Bloch, and A. Amo, “Semi-dirac transport and anisotropic localization in polariton honeycomb lattices,” *Phys. Rev. Lett.* **125**, 186601 (2020).
 - 30 P. Sharma, A. Principi, and D. L. Maslov, “Optical conductivity of a dirac-fermi liquid,” *Phys. Rev. B* **104**, 045142 (2021).
 - 31 V. V. Cheianov and V. I. Fal’ko, “Friedel Oscillations, impurity scattering, and temperature dependence of resistivity in graphene,” *Phys. Rev. Lett.* **97**, 226801 (2006).
 - 32 G. W. Semenoff, “Chiral symmetry breaking in graphene,” *Phys. Scr.* **T146**, 014016 (2012).
 - 33 Gerald D. Mahan, *Many-Particle Physics* (Springer US, Boston, 2000).
 - 34 T. A. Sedrakyan and M. E. Raikh, “Magneto-oscillations due to electron-electron interactions in the ac conductivity of a two-dimensional electron gas,” *Phys. Rev. Lett.* **100**, 086808 (2008).
 - 35 I. L. Aleiner and K. B. Efetov, “Effect of disorder on transport in graphene,” *Phys. Rev. Lett.* **97**, 236801 (2006).
 - 36 A. Altland, “Low-energy theory of disordered graphene,” *Phys. Rev. Lett.* **97**, 236802 (2006).
 - 37 P. M. Ostrovsky, I. V. Gornyi, and A. D. Mirlin, “Electron transport in disordered graphene,” *Phys. Rev. B* **74**, 235443 (2006).
 - 38 T. A. Sedrakyan, E. G. Mishchenko, and M. E. Raikh, “Smearing of the two-dimensional Kohn Anomaly in a non-quantizing magnetic field: Implications for interaction effects,” *Phys. Rev. Lett.* **99**, 036401 (2007).
 - 39 See Supplementary Materials. It contains the detailed derivation of the static longitudinal conductivity from Kubo formula.
 - 40 E. H. Hwang and S. Das Sarma, “Acoustic phonon scattering limited carrier mobility in two-dimensional extrinsic graphene,” *Phys. Rev. B* **77**, 115449 (2008).
 - 41 S. Fratini and F. Guinea, “Substrate-limited electron dynamics in graphene,” *Phys. Rev. B* **77**, 195415 (2008).
 - 42 D. L. Nika and A. A. Balandin, “Two-dimensional phonon transport in graphene,” *Journal of Physics: Condensed Matter* **24**, 233203 (2012).
 - 43 J. H. Seol, I. Jo, A. L. Moore, L. Lindsay, Z. H. Aitken, M. T. Pettes, X. Li, Z. Yao, R. Huang, D. Broido, N. Mingo, R. S. Ruoff, and L. Shi, “Two-dimensional phonon transport in supported graphene,” *Science* **328**, 213 (2010).
 - 44 L. Banszerus, M. Schmitz, S. Engels, J. Dauber, M. Oellers, F. Haupt, K. Watanabe, T. Taniguchi, B. Beschoten, and C. Stampfer, “Ultrahigh-mobility graphene devices from chemical vapor deposition on reusable copper,” *Science Advances* **1**, e1500222 (2015).
 - 45 Gábor Zala, B.N. Narozhny, and I.L. Aleiner, “Interaction corrections to the hall coefficient at intermediate temperatures,” *Phys. Rev. B* **64**, 201201 (2001).

Supplemental Material: Ballistic magnetotransport in graphene

I. STATIC CONDUCTIVITY

In this section, we present the definitions and the main formulas for static conductivity. The Dirac electron in graphene, coupled to $U(1)$ gauge field, is described by the Hamiltonian,

$$\hat{H}_0 = v_F \int d^2\mathbf{r} \hat{\Psi}^\dagger(\mathbf{r}) [\Sigma_\alpha (-i\partial^\alpha + eA^\alpha)] \hat{\Psi}(\mathbf{r}). \quad (\text{S1})$$

Here a summation is assumed over the repeating index, α , with $\alpha = x, y$, v_F is the Fermi velocity, $\hat{\Psi} = (\hat{\psi}_{AK}, \hat{\psi}_{BK}, \hat{\psi}_{BK'}, \hat{\psi}_{AK'})$ is the 4-component fermion operator. The four-dimensional matrix $\Sigma_{x,y} = \tau_z \otimes \sigma_{x,y}$, where τ_z is the third Pauli matrix acting on K, K' space and $\sigma_{x,y}$ are Pauli matrices acting on the space of A, B sublattices. Then the current operator for Dirac electrons is given by $ev_F \hat{\Psi}^\dagger(\mathbf{r}) \Sigma_\alpha \hat{\Psi}(\mathbf{r})$.

Now consider the system with the disorder potential $V_{\text{imp}}(\mathbf{r})$ and the interaction potential $U(\mathbf{r})$. We assume the correlation of the disorder potential is point-like. Namely,

$$\begin{aligned} \langle V_{\text{imp}}(\mathbf{r}) \otimes V_{\text{imp}}(\mathbf{r}') \rangle_I = \delta_{\mathbf{r},\mathbf{r}'} & \left[\gamma_0 \mathbf{1}_4 \otimes \mathbf{1}_4 + \beta_\perp \Sigma_{x,y} \Lambda_{x,y} \otimes \Sigma_{x,y} \Lambda_{x,y} \right. \\ & \left. + \gamma_\perp \Sigma_{x,y} \Lambda_z \otimes \Sigma_{x,y} \Lambda_z + \beta_z \Sigma_z \Lambda_{x,y} \otimes \Sigma_z \Lambda_{x,y} + \gamma_z \Sigma_z \Lambda_z \otimes \Sigma_z \Lambda_z \right] \end{aligned} \quad (\text{S2})$$

The bracket $\langle \dots \rangle_I$ is the average over impurity distributions. Matrices above are defined by $\Sigma_z = \tau_0 \otimes \sigma_z$, $\Lambda_x = \tau_x \otimes \sigma_x$, $\Lambda_y = \tau_y \otimes \sigma_y$, $\Lambda_z = \tau_z \otimes \sigma_z$. The $\gamma_0, \beta_\perp, \gamma_\perp, \beta_z$ and γ_z describe the strength of disorder potential.

According to the Kubo formula, the static conductivity is estimated by the current-current correlation function, $\sigma_{\alpha,\beta} = \lim_{\omega \rightarrow 0} \frac{i}{\omega} \Pi_{\alpha,\beta}(\omega)$. Here the $\Pi_{\alpha,\beta}(\omega)$ is obtained by taking analytic continuation of $\Pi_{\alpha,\beta}(i\Omega_n)$ via $i\Omega_n \rightarrow \omega$,

$$\Pi_{\alpha,\beta}(i\Omega_n) = \int_0^{1/T} d\tau \langle T_\tau \hat{j}_\alpha(\tau) \hat{j}_\beta(0) \rangle e^{i\Omega_n \tau} \quad (\text{S3})$$

Here $\hat{j}_\alpha(\tau)$, $\alpha = 1, 2$, is the current operator at imaginary time τ , $\omega_n = 2\pi T n$ is the bosonic Matsubara frequency and $i\Omega_n \rightarrow \omega$ represents the analytic continuation.

We treat the electron-electron interaction as the perturbation to H_0 . The current-current correlation function can be generally expressed by

$$\Pi_{\alpha,\beta}(i\Omega_n) = -T \sum_{i\omega_m} J_\alpha G(i\omega_m) J_\beta G(i\omega_m - i\Omega_n) - T \sum_{i\omega_m} J_\alpha G(i\omega_m) \Gamma_\beta(i\omega, i\omega - i\Omega_n) G(i\omega_m - i\Omega_n) \quad (\text{S4})$$

where $\omega_m = (2\pi m + 1)T$ is the fermionic Matsubara frequency and Γ is the vertex correction. The current operator of Dirac electrons J_α above reads $J_\alpha = ev_F \Sigma_\alpha$. Here G is the exact green function for the interacting system. The first term in the RHS is of the self-energy type and the second term contains the vertex correction. Below we refer to the self-energy/vertex-type contributions to $\sigma_{\alpha,\beta}$ as to $\sigma_{\alpha,\beta}^{S/V}$.

A. Self energy correction

The standard analytic continuation procedure transform the summation over Matsubara frequency in $\sigma_{\alpha,\beta}^S$ into a single variable integral,

$$\sigma_{\alpha,\beta}^S = \frac{1}{4\pi} \text{Re} \int_{-\infty}^{+\infty} d\epsilon \partial_\epsilon \left[\tanh \frac{\epsilon}{2T} \right] \left[J_\alpha G_R(\epsilon) J_\beta G_A(\epsilon) - J_\alpha G_R(\epsilon) J_\beta G_R(\epsilon) \right]. \quad (\text{S5})$$

Here $G_{R/A}$ is the retarded/advanced Green's function. Consider the first order perturbation over the interactions. There are two types of diagrams, Hartree and Fock. The diagrams *a* and *b* in Fig. 3 are of the Fock type. Here, we only focus on the calculation of Fock self energy, $\Sigma_F(i\omega_m) = T \sum_{i\nu_l} G_0(i\omega_m - i\nu_l) V(i\nu_l)$. Here ν_l is the bosonic Matsubara frequency, G_0 is the Green's function for non-interacting Hamiltonian H_0 and $V(i\nu_l)$ is the interaction potential in the frequency space (up to first order in perturbation, $V(i\nu_l)$ is simply constant V , not depending on frequencies). Inserting the self-energy Σ_F into Eq. S5 and performing analytic continuation, one obtains

$$\begin{aligned} \sigma_{\alpha,\beta}^S \simeq \frac{V}{4\pi^2} \text{Im} \int d\Omega \frac{d}{d\Omega} \left(\Omega \coth \frac{\Omega}{2T} \right) & \left[J_\alpha G_R(\epsilon) V(\Omega) G_A(\epsilon - \Omega) G_R(\epsilon) J_\beta G_A(\epsilon) \right. \\ & \left. - J_\alpha G_R(\epsilon) V(\Omega) G_R(\epsilon - \Omega) G_R(\epsilon) J_\beta G_A(\epsilon) - J_\alpha G_R(\epsilon) V(\Omega) G_A(\epsilon - \Omega) G_R(\epsilon) J_\beta G_R(\epsilon) \right]. \end{aligned} \quad (\text{S6})$$

B. Vertex correction

Similarly, one could perform the analytic continuation in the vertex correction and find

$$\sigma_{\alpha,\beta}^V = \frac{T}{4\pi} \text{Re} \int d\epsilon \left[\partial_\epsilon \tanh \frac{\epsilon}{2T} \right] J_\alpha \left[G_R(\epsilon) \Gamma_\beta(\epsilon + i\delta, \epsilon - i\delta) G_A(\epsilon) - G_R(\epsilon) \Gamma_\beta(\epsilon + i\delta, \epsilon + i\delta) G_R(\epsilon) \right], \quad (\text{S7})$$

where δ is an arbitrary small positive number. Diagrams *c* and *d* in Fig. 3 are of the vertex type. The first order vertex correction reads $\Gamma_\beta(i\omega_m, i\omega_m - i\nu_n) = VT \sum_{i\nu_l} G_0(i\omega_m - i\nu_l) J_\beta G_0(i\omega_m - i\nu_l - i\nu_n)$. Performing the analytic continuation for $i\omega$, $i\nu$ and inserting Γ into Eq. S7, one finds

$$\sigma_{\alpha,\beta}^V \simeq \frac{1}{8\pi^2} \text{Im} \int d\Omega \frac{d}{d\Omega} \left(\Omega \coth \frac{\Omega}{2T} \right) \times J_\alpha \left[2G_R(\epsilon) V(\Omega) G_A(\epsilon - \Omega) J_\beta G_A(\epsilon - \Omega) G_A(\epsilon) - G_R(\epsilon) V(\Omega) G_A(\epsilon - \Omega) J_\beta G_A(\epsilon - \Omega) G_R(\epsilon) \right]. \quad (\text{S8})$$

II. CALCULATION OF THE STATIC LONGITUDINAL CONDUCTIVITY

This section provides a detailed calculation to derive the main temperature dependence in the static longitudinal conductivity, $\delta\sigma$. The Fock-type diagrams, including impurity scatterings, are shown in Fig. 3. Taking all four diagrams into consideration, we find that the leading correction to σ in the ballistic regime ($T\tau \gg 1$) is given by

$$\delta\sigma \simeq \frac{V}{2\pi^2} \text{Im} \int d\Omega \frac{d}{d\Omega} \left(\Omega \coth \frac{\Omega}{2T} \right) \text{tr} \left[J_\alpha G_R(\epsilon) V_{\text{imp}} G_R(\epsilon) V(\Omega) G_A(\epsilon - \Omega) V_{\text{imp}} G_A(\epsilon - \Omega) G_R(\epsilon) J_\beta G_A(\epsilon) \right]. \quad (\text{S9})$$

Here V_{imp} represents the impurity potential. Thus the main task is to evaluate the Eq. S9. Here we adopt the semiclassical limit to estimate Eq. S9. In the semiclassical limit, the interaction potential acts as a touching potential. The real space Green's function averaged over impurities, reads

$$\langle G(\mathbf{r}, \omega) \rangle_I = \frac{k_F}{2v_F} \sqrt{\frac{1}{2k_F r}} e^{i \text{sgn}(\omega) \Phi_0(r) - r/(2rv_F)} M, \quad (\text{S10})$$

where the phase $\Phi_0(r) = k_F r + \omega r/v_F + \pi/4 - r^3/(24k_F l^4)$ and the matrix M is given by

$$M(\mathbf{r}, \text{sgn}(\omega)) \simeq (\text{sgn}(\omega) + i(2k_F r)^{-1}) \hat{r} \cdot \boldsymbol{\Sigma} + \hat{I} - i \text{sgn}(\omega) \varphi(r) \hat{\Sigma}_z - \frac{\varphi(r)^2}{2} \hat{I}, \quad (\text{S11})$$

where $\boldsymbol{\Sigma} = (\Sigma_x, \Sigma_y)$ and \hat{I} is the identity matrix. Here $\varphi(r) = \omega_0 r/(2v_F)$ is the half of the angle corresponding to the arc of the Larmor circle with length r . The angle $\varphi(r)$ represents the extent of the chiral symmetry breaking, since Σ_z anti-commutes with $\Sigma_{x,y}$.

To perform real space integration in the expression for the conductivity, one may make use of the following identity

$$\int d^2x G_R(\mathbf{x}', \mathbf{x}; \epsilon) \hat{\Sigma}_\alpha G_A(\mathbf{x}, \mathbf{y}; \epsilon) = -\frac{i\tau}{k_F} \frac{\partial}{\partial x'_\alpha} \left[G_A - G_R \right](\mathbf{x}', \mathbf{y}; \epsilon), \quad (\text{S12})$$

where $\alpha = 1, 2$. This identity helps us in Eq. S9 bringing the convolution of two propagators into one around the vertex. Applying Eq. S12 twice (once for J_α and once for J_β), one arrives at

$$\delta\sigma \simeq -\frac{e^2 \tau^2 k_F^2}{64\pi^2 v_F^2 y^2} \frac{1}{2\pi^2} \text{Im} \int d\Omega \frac{d}{d\Omega} \left(\Omega \coth \frac{\Omega}{2T} \right) \text{tr} \int d^2y \hat{u} M(-\mathbf{y}; +) M(\mathbf{y}; -) \hat{u} M(-\mathbf{y}; -) M(\mathbf{y}; +) e^{2i(\Omega + i/\tau)y/v_F}.$$

Here \hat{u} is a 4×4 matrix and $\hat{u} \otimes \hat{u}$ inherits the matrix structure from Eq. S2. Namely, it corresponds to the part contained in the square bracket of Eq. S2. To further evaluate $\delta\sigma$, one needs to perform angular integration yielding

$$\text{tr} \int d\theta \hat{u} M(-\mathbf{y}; +) M(\mathbf{y}; -) \hat{u} M(-\mathbf{y}; -) M(\mathbf{y}; +) = 32\pi \left(2p \sin^2 \varphi(y) + t \right). \quad (\text{S13})$$

Here θ is the angular coordinate of \mathbf{y} . Parameters are defined as $p' = \gamma_0 - \beta_z - \gamma_z$ and $t' = 2\gamma_z + 2\beta_z + \beta_\perp + \gamma_\perp$. Linearly expanding $\sin \varphi$, one can write $\delta\sigma$ as the following single variable integral

$$\delta\sigma \simeq -\frac{e^2 \tau^2 k_F^2}{4\pi^3 v_F^2} \int d\Omega \frac{d}{d\Omega} \left(\Omega \coth \frac{\Omega}{2T} \right) \text{Im} \int \frac{dy}{y} \left(p' \frac{y^2}{2k_F^2 l^4} + t' \right) e^{2i(\Omega + i/\tau)y/v_F}. \quad (\text{S14})$$

Now we handle the integral over y firstly and define

$$I(B) = \text{Im} \int \frac{dy}{y} \left(p' \frac{y^2}{2k_F^2 l^4} + t' \right) e^{2i(\Omega + i\tau)y/v_F}. \quad (\text{S15})$$

The zero field result is simply given by

$$I(0) \simeq t' \int_{1/k_F}^{\infty} dy \frac{1}{y} \sin \frac{2\Omega y}{v_F} = \frac{\pi t'}{2} + O(\Omega/E_F). \quad (\text{S16})$$

Note that the scalar part α_0 of impurity potential does not contribute to t , i.e., the zero field conductivity. The field-dependent contribution reads

$$I(B) - I(0) = \frac{p'}{2k_F^2 l^4} \int_{1/k_F}^{v_F/\omega_0} y \sin \frac{2\Omega y}{v_F} e^{-\frac{2y}{v_F\tau}} dy. \quad (\text{S17})$$

We limit our attention to the limit $\omega_0\tau \ll 1$ so that $\exp(-(\omega_0\tau)^{-1}) \simeq 0$. This ensures the convergence of the integral. Also $E_F\tau \gg 1$ is assumed. Then we define $x = 2y/v_F\tau$ and rewrite the integral as

$$I(B) - I(0) \simeq \frac{p'}{8k_F^2 l^4} (v_F\tau)^2 \int_0^{+\infty} x \sin(\Omega\tau x) e^{-x} dx. \quad (\text{S18})$$

Here the lower cut-off is set as zero and the upper cut-off is set to be infinity, since $1/(E_F\tau) \ll 1$ and $1/(\omega_0\tau) \gg 1$. Performing the integral, one obtains

$$I(B) - I(0) = p' \frac{(v_F\tau)^2}{8k_F^2 l^4} \frac{2\Omega\tau}{(1 + \Omega^2\tau^2)^2}. \quad (\text{S19})$$

Thus, with the help of Eqs. S16 and S19, one can write the conductivity as a single variable integral

$$\delta\sigma \simeq -\frac{e^2\tau^2 k_F^2}{4\pi^3 v_F^2} \int d\Omega \frac{d}{d\Omega} \left(\Omega \coth \frac{\Omega}{2T} \right) \left[\frac{\pi t'}{2} + p' \frac{(v_F\tau)^2}{4k_F^2 l^4} \frac{\Omega\tau}{(1 + \Omega^2\tau^2)^2} \right]. \quad (\text{S20})$$

The remaining task is to simply evaluate the integral above. Now we treat the zero-field and field-dependent contributions separately

- **Zero-field contribution.** At $B = 0$, the integral involved is

$$\int_0^{E_F} d\Omega \frac{d}{d\Omega} \left(\Omega \coth \frac{\Omega}{2T} \right) = \left[E_F \coth(E_F/2T) - 2T \right].$$

Here we set the upper bound for Ω to be the Fermi energy, E_F . This integral was performed in Ref. S45 and leads to the well-known linear temperature dependence in the longitudinal conductivity. Since $E_F/T \gg 1$, the temperature dependence in $\coth(E_F/2T)$ function is exponentially weak. The main temperature dependence comes from the latter, the linear one $-2T$.

- **Field-dependent contribution.** The field-dependent contribution is given by the integral

$$\int d\Omega \frac{d}{d\Omega} \left(\Omega \coth \frac{\Omega}{2T} \right) \frac{\Omega\tau}{(1 + \Omega^2\tau^2)^2} = 2T \int_0^{\infty} dz \frac{d}{dz} \left(z \coth z \right) \frac{2z \times T\tau}{(1 + 4z^2(T\tau)^2)^2}. \quad (\text{S21})$$

Here we define the variable $z = \Omega/2T$. Since we consider the ballistic regime, we only need the asymptotic behavior of the integral at $T\tau \gg 1$. We find that Eq. S21 has the asymptotic behavior, $\alpha 2T(T\tau)^{-2}$ when $T\tau \gg 1$. Here α is analytically found to be $\alpha = \pi/24$. The functional dependence $\propto (T\tau)^{-2}$ and α are derived below.

For the integrand in the Eq. S21, one can separate the integral domain into two parts. They are $(0, \kappa)$ and (κ, ∞) for variable z with $\kappa \sim 1$. We call each region's contribution to the integral as J_1, J_2 in a sequence. At the first region, $\partial_z(z/\tanh z) \simeq 2z/3$. Then one defines $x = 2zT\tau$ and gets

$$J_1 = 2T \frac{(T\tau)^{-2}}{6} \int_0^{+\infty} dx \frac{x^2}{(1+x^2)^2} = \frac{\pi}{24} 2T(T\tau)^{-2}. \quad (\text{S22})$$

Here we extend the upper bound of integral $2T\tau$ to ∞ , since $T\tau \gg 1$ and we are looking for the leading order. In second region, $\partial_z(z/\tanh z) \simeq 1$. One similarly obtains

$$J_2 \simeq 2T \int_{\kappa}^{\infty} dz (2zT\tau)^{-3} \propto (T\tau)^{-3}. \quad (\text{S23})$$

From the analysis, one can clearly see that J_1 and J_2 give the leading contributions and the asymptotic behavior of Eq. S21 is $\sim (T\tau)^{-2}$.

Now we assume the weak and short-ranged scatterer and identify the expression of τ in the Born-approximation^{S37},

$$\frac{1}{\tau} = \frac{k_F}{2v_F} (\gamma_0 + 4\beta_{\perp} + 2\gamma_{\perp} + 2\beta_z + \gamma_z). \quad (\text{S24})$$

Thus $\delta\sigma$ can be simplified to be

$$\delta\sigma \simeq \lambda \frac{e^2\tau}{\pi} \left(\tilde{t}T - \tilde{p} \frac{\omega_0^2}{48T} \right). \quad (\text{S25})$$

Here λ is the dimensionless interaction parameter $\lambda = U_0 k_F (2\pi v_F)^{-1}$. Parameters \tilde{t} and \tilde{p} are dimensionless and describe the strength of disorder potential. They are defined by

$$\tilde{t} = \frac{2\gamma_z + 2\beta_z + \beta_{\perp} + \gamma_{\perp}}{\gamma_0 + 4\beta_{\perp} + 2\gamma_{\perp} + 2\beta_z + \gamma_z}, \quad \tilde{p} = \frac{\gamma_0 - \beta_z - \gamma_z}{\gamma_0 + 4\beta_{\perp} + 2\gamma_{\perp} + 2\beta_z + \gamma_z}. \quad (\text{S26})$$

Eq. S25 is the main conclusion in this note. (i) The zero-field contribution linearly depends on the temperature, and this linear dependence is highly sensitive to the nature of the disorder. Once the impurity potential is scalar-like, i.e., only $\alpha_0 \neq 0$ while $\gamma_z = \beta_z = \beta_{\perp} = \gamma_{\perp} = 0$, the linear in temperature term vanishes. This is consistent with the result in Ref. S31. (ii) The field-dependent correction is inversely dependent on the temperature. If the impurity potential is scalar-like, the ω_0^2/T gives the leading interaction correction to the conductivity.